



Original article

Substituted 4-phenyl-2-aminoimidazoles and 4-phenyl-4,5-dihydro-2-aminoimidazoles as voltage-gated sodium channel modulators



Nace Zidar^a, Žiga Jakopin^a, David J. Madge^b, Fiona Chan^b, Jan Tytgat^c, Steve Peigneur^c, Marija Sollner Dolenc^a, Tihomir Tomašić^a, Janez Ilaš^a, Lucija Peterlin Mašič^a, Danijel Kikelj^{a,*}

^a University of Ljubljana, Faculty of Pharmacy, Aškerčeva 7, 1000 Ljubljana, Slovenia

^b Xention Limited, Iconix Park, London Road, Pampisford, Cambridge CB22 3EG, UK

^c University of Leuven (KU Leuven), Toxicology & Pharmacology, O&N2, PO Box 922, Herestraat 49, 3000 Leuven, Belgium

ARTICLE INFO

Article history:

Received 7 November 2013

Received in revised form

16 December 2013

Accepted 22 December 2013

Available online 3 January 2014

Keywords:

Voltage-gated sodium channel

Nav channel modulator

Marine alkaloid

Clathrocin

Pyrrole-2-aminoimidazole

4-Phenyl-2-aminoimidazole

ABSTRACT

Voltage-gated sodium channels play an integral part in neurotransmission and their dysfunction is frequently a cause of various neurological disorders. On the basis of the structure of marine alkaloid clathrocin, twenty eight new analogs were designed, synthesized and tested for their ability to block human Nav1.3, Nav1.4 and Nav1.7 channels, as well as for their selectivity against human cardiac isoform Nav1.5, using automated patch clamp electrophysiological assay. Several compounds exhibited promising activities on different Nav channel isoforms in the medium micromolar range and some of the compounds showed also moderate isoform selectivities. The most promising results were obtained for the Nav1.3 channel, for which four compounds were found to possess IC₅₀ values lower than 15 μM. All of the active compounds bind to the open-inactivated states of the channels and therefore act as state-dependent modulators. The obtained results validate the approach of using natural products driven chemistry for drug discovery starting points and represent a good foundation for future design of selective Nav modulators.

© 2013 Elsevier Masson SAS. All rights reserved.

1. Introduction

Voltage-gated sodium channels (VGSC, Nav channels) are integral membrane proteins which play essential roles in the initiation and propagation of action potentials in neurons and other electrically excitable cells. They are composed of a single α -subunit which forms a voltage-sensing pore and one or more auxiliary β -subunits. To date, nine different α -subunits (Nav1.1–Nav1.9) and four different β -subunits have been identified. The VGSC isoforms are distributed differentially throughout the electrically excitable cells of the body, and have different functional properties according to their role in each tissue type. Nav1.1–1.3 and Nav1.6 are mainly expressed in the central nervous system, Nav1.4 in the skeletal

muscle, Nav1.5 in the heart, and Nav1.7–1.9 are characteristic of the peripheral nervous system [1–7].

The abnormally increased activity of sodium channels leads to over-excitation of specific groups of cells which can cause different neurodegenerative diseases, chronic pain, epilepsy, arrhythmias and spasticity. Mutations of Nav channel genes and their encoded proteins have been identified in heart, brain, skeletal muscle and peripheral nerves [8–11]. Both, gain and loss of function mutations in Nav1.1 and Nav1.2 can give rise to epilepsy [12,13] and migraine [14]. A number of preclinical studies have implicated Nav1.3, Nav1.7, Nav1.8 and Nav1.9 in nociceptive processing [15,16] and mutations in their genes were linked to spontaneous chronic pain. Mutations of Nav1.4 that result in hyperactive skeletal sodium channels have been shown to cause myotonia or flaccid paralysis [17], whereas mutations of Nav1.5 have profound effects on cardiac function, leading to a range of cardiac abnormalities [18]. Owing to the extremely broad therapeutic potential of VGSC modulators, and to the recently disclosed first X-ray crystal structures of bacterial Nav channels [1–3], discovery of VGSC modulators has become one of the most attractive topics in medicinal chemistry.

Although there are several drugs acting at Nav channels, e.g. local anesthetics (lidocaine, procaine), antiarrhythmics (lidocaine,

Abbreviations: VGSC, voltage-gated sodium channel; Nav channel, voltage-gated sodium channel; TBTU, *N,N,N',N'*-tetramethyl-*O*-(benzotriazol-1-yl)uronium tetrafluoroborate; DMAP, 4-(dimethylamino)pyridine; NMM, *N*-methylmorpholine; Pro, proline; THF, tetrahydrofuran; DMF, *N,N*-dimethylformamide; DMAP, 4-dimethylaminopyridine; TFA, trifluoroacetic acid; ESI, electrospray ionization; Boc₂O, di-*tert*-butyl dicarbonate; Boc, *tert*-butoxycarbonyl.

* Corresponding author. Tel.: +386 1 4769561; fax: +386 1 4258031.

E-mail address: danijel.kikelj@ffa.uni-lj.si (D. Kikelj).

tocainide, mexiletine) and antiepileptics (phenytoin, carbamazepine, lamotrigine), a more rational approach is required to exploit the full therapeutic potential of these drug targets. Current drugs acting on Na_v channels have low potency and are relatively non-selective, therefore there is a need for the development of isoform-selective modulators which offers the promise of significant advantage over current therapeutic agents [9,19,20]. Recent studies show promise that small molecules can be made selective for different Na_v channel isoforms [8,9,21–25]. Relatively favorable side effect profiles of some currently used drugs acting on Na_v channels are generally attributed to their state-dependent action. They usually have a much higher affinity for inactivated channels compared to resting channels, therefore their IC₅₀ values are several hundred times higher on hyperpolarized VGSCs than on VGSCs in depolarized membranes [26,27]. This state-dependency of action is therefore considered to be a key predictor of a high therapeutic index for a VGSC blocker.

The marine ecosystem is a rich source of chemically and functionally diverse toxins that interact with Na_v channels and provide inspiration for drug design [28,29]. Alkaloids from the Caribbean sponges of the genus *Agelas*, e.g. monomers clathrocin, hymenidin and oroidin, and dimers sceptrin and dibromosceptrin (Fig. 1), have been shown to interact with muscle and nerve membrane receptors and channels, including VGSCs. Electrophysiological studies suggested that clathrocin and dibromosceptrin act on Na_v channels by influencing channel ion conductance, and by modifying the channel inactivation characteristics, respectively [30]. These alkaloids belong to the pyrrole-2-aminoimidazole structural class of marine alkaloids, with intriguing structural complexity and diverse biological activities [31,32]. In contrast to the majority of neurotoxins, which have high molecular weights and many chiral centers leading to complex 3D architectures, the structures of clathrocin-like alkaloids are relatively simple. This makes them suitable candidates for optimization using established medicinal chemistry strategies. Due to their favorable size and physicochemical properties, they have the potential to permeate further into the channel and possibly bind to sites which are not available to large toxin molecules [9].

The design of the present series of compounds was based on the structure of the alkaloid clathrocin and is schematically presented in Fig. 2. The molecule of clathrocin consists of a 2-aminoimidazole moiety that is connected to a pyrrole ring with a 5-atom long, partially flexible, linker. This linker gives clathrocin a certain extent of conformational freedom which is not optimal for the binding affinity. In addition, the linker contains in its structure a C=C double bond conjugated to the 2-aminoimidazole ring that can undergo various transformations, such as additions of different nucleophiles [33] or Diels–Alder cycloadditions [34,35]. The aim of the present study was to design derivatives with a conformationally restricted central part of the molecule that would at the same time lack the potentially unstable alkenyl

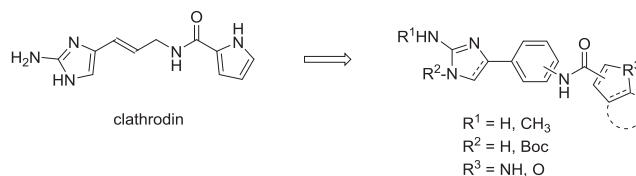


Fig. 2. Design of substituted 4-phenyl-2-aminoimidazoles and 4-phenyl-4,5-dihydro-2-aminoimidazoles as conformationally restricted clathrocin analogs.

double bond. To achieve these goals, we decided to introduce a phenyl ring at position 5 of the 2-aminoimidazole moiety so that the length of the molecule would remain unchanged. To explore the correct spatial arrangement of functional groups we designed two sets of compounds, one with 1,3- and the other with 1,4-substitution patterns on the phenyl ring. In addition to the 2-substituted pyrrole ring present in the clathrocin molecule, analogs with pyrrol-3-yl, furan-2-yl, indol-2-yl, indol-3-yl, (*R*)-pyrrolidin-2-yl or (*S*)-pyrrolidin-2-yl substituents were prepared. To assess the importance of the free amino group of the 2-aminoimidazole ring, we designed compounds **24–32** with an *N*-methyl substituent in position 2 (Schemes 4 and 5). In addition, to examine whether aromaticity and planarity of the imidazole ring are important for biological activity, a set of 4,5-dihydro-2-aminoimidazoles **27–32** with a reduced imidazole C=C bond was prepared (Scheme 5).

2. Results and discussion

2.1. Chemistry

The synthetic route towards the key intermediates **4a**, **4b** and compound **6** is presented in Scheme 1. 2-Bromo-3-nitroacetophenone or 2-bromo-4-nitroacetophenone was reacted with 2-aminopyrimidine and a catalytic amount of 4-dimethylamino pyridine in acetonitrile to afford the pyrimidinium salts **1a** or **1b**, respectively. A dehydrated compound **1c** was formed instead of **1a**, when the reaction of 2-aminopyrimidine and 2-bromo-3-nitroacetophenone was carried out at 85 °C instead of at room temperature. This can probably be attributed to the electron withdrawing effect of the nitro group on the phenyl ring, which is more prominent when the nitro group is in the *para* position (compound **1b**) than in the *meta* position (compound **1a**). Hydrazinolysis of compounds **1a–c** in ethanol using microwave irradiation, followed by a Dimroth-type rearrangement resulted in formation of substituted 2-aminoimidazoles **2a** and **2b**. Both steps were accomplished following a literature procedure [36] where detailed mechanisms of the reactions are described. In a first attempt to prepare derivatives with carboxamido substituents on the phenyl ring, after reduction of the nitro group of **2a** by catalytic

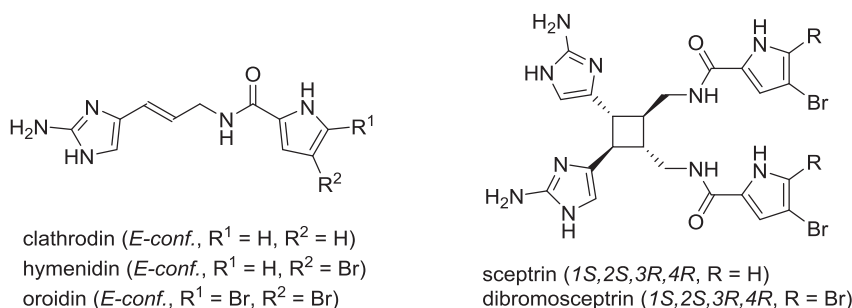
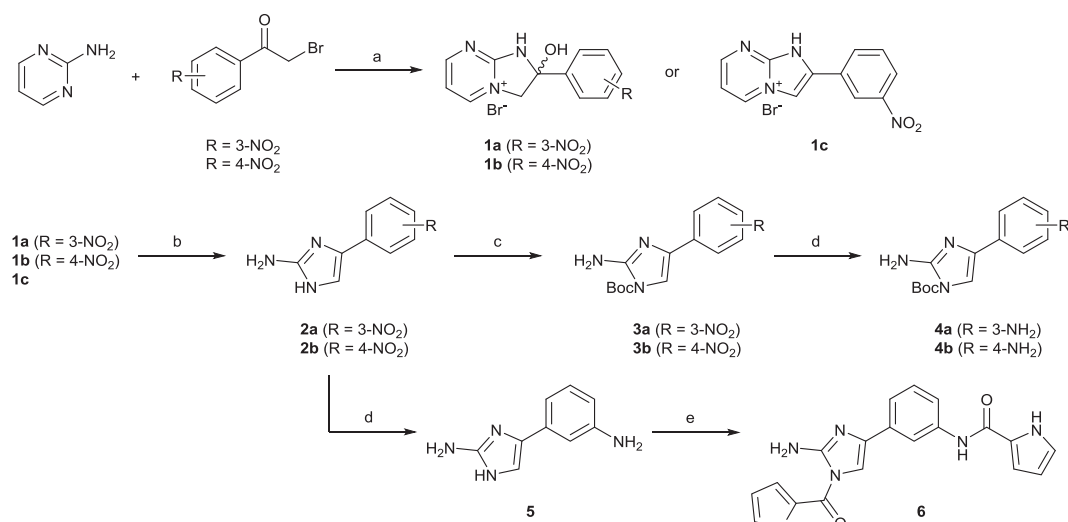


Fig. 1. Structures of *Agelas* alkaloids clathrocin, hymenidin, oroidin, sceptrin and dibromosceptrin.

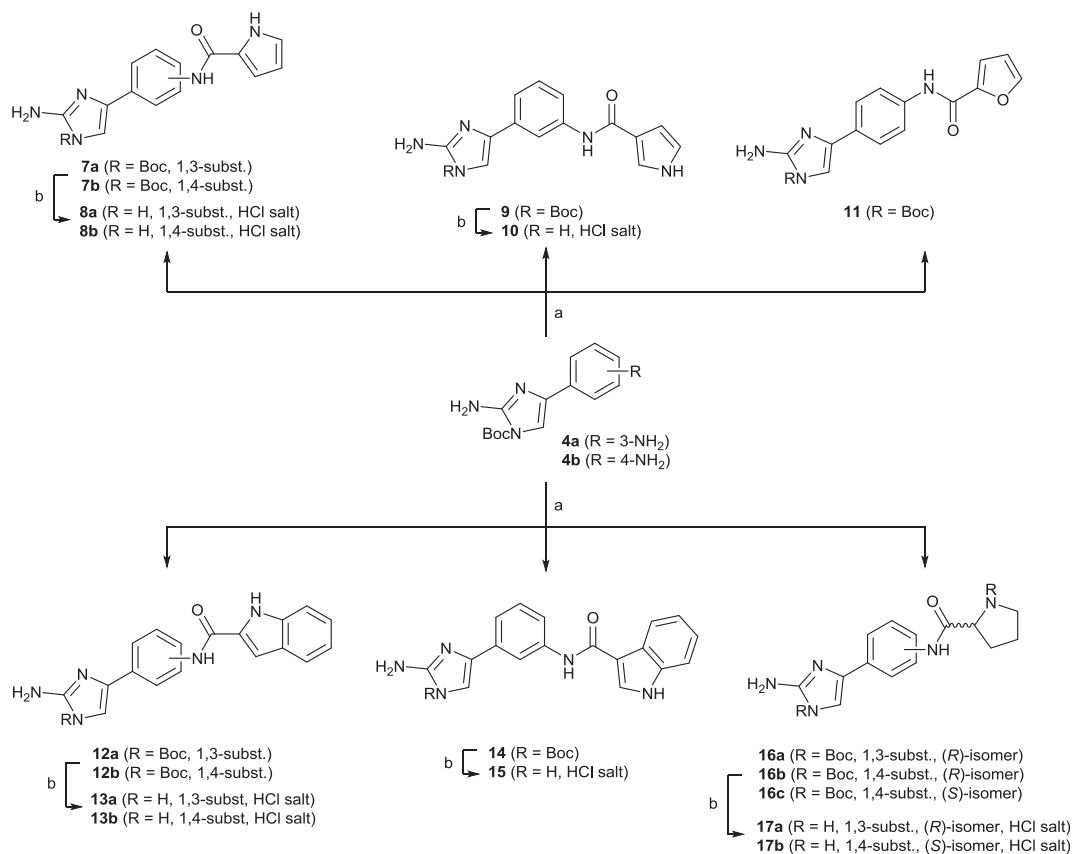


Scheme 1. Synthesis of key intermediates **4a** and **4b**, and compound **6**. *Reagents and conditions:* (a) method 1: DMAP, CH_3CN , rt, 5 h (for the synthesis of **1a** and **1b**); method 2: DMAP, CH_3CN , 85°C , 5 h (for the synthesis of **1c**); (b) hydrazine hydrate, EtOH, MW, 120°C , 40 min; (c) Boc₂O, 2:1 MeOH/ H_2O , rt, 3 h; (d) $\text{H}_2/\text{Pd}-\text{C}$, THF, rt, 5 h; (e) 1 equiv pyrrole-2-carboxylic acid, TBTU, NMM, DMF, rt, 15 h.

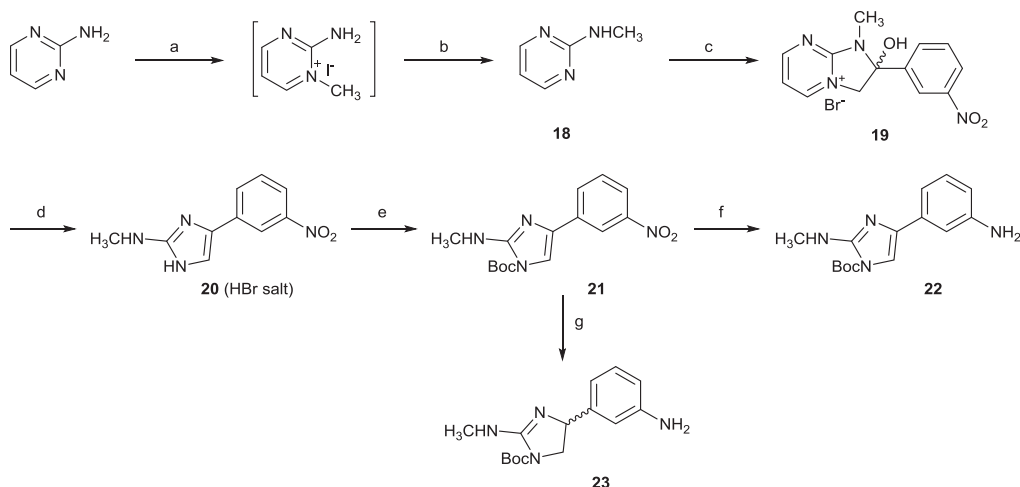
hydrogenation, the obtained amine **5** was coupled with pyrrole-2-carboxylic acid in a TBTU-promoted reaction. We found that coupling occurred at two possible sites, the aromatic amino group and the imidazole N-1, to give the product **6**. Interestingly, the reaction did not occur at the 2-amino group of the imidazole ring, probably because of its low reactivity. Therefore, the imidazole N-1 nitrogen was Boc-protected by reacting compounds **2a** and **2b** with

Boc-anhydride in a mixture of methanol and water. The reduction of the nitro group of Boc-protected derivatives **3a** and **3b** was accomplished through catalytic hydrogenation in tetrahydrofuran using Pd-C as a catalyst, to give the target amines **4a** and **4b**.

The 4-phenyl-2-aminoimidazole analogs **7–17** were prepared according to Scheme 2. TBTU-promoted coupling of **4a** or **4b** and the corresponding carboxylic acid (pyrrole-2-carboxylic acid,



Scheme 2. Synthesis of 4-phenyl-2-aminoimidazoles **7–17**. *Reagents and conditions:* (a) corresponding carboxylic acid, TBTU, NMM, CH_2Cl_2 , 35°C , 24 h; (b) method 1: $\text{HCl}_{(\text{g})}$, THF/EtOH, rt, 5 h (for the synthesis of **8a**, **10**, **13a**, **15** and **17a**); method 2: acetyl chloride, EtOH, 0°C , 1 h (for the synthesis of **8b**, **13b** and **17b**).



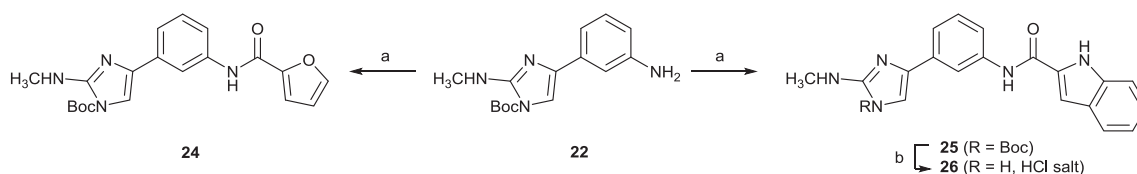
Scheme 3. Synthesis of *N*-methylated intermediates **22** and **23**. *Reagents and conditions:* (a) CH_3I , acetone, 75°C , 15 h; (b) NaOH , $\text{EtOH}/\text{H}_2\text{O}$, 80°C , 0.5 h; (c) 2-bromo-3-nitroacetophenone, DMAP, CH_3CN , 50°C , 15 h; (d) hydrazine hydrate, EtOH , MW: 120°C , 40 min; (e) Boc_2O , 2:1 $\text{MeOH}/\text{H}_2\text{O}$, rt, 3 h; (f) $\text{H}_2/\text{Pd}-\text{C}$, THF, rt, 5 h; (g) $\text{H}_2/\text{Pd}-\text{C}$, THF, rt, 24 h.

pyrrole-3-carboxylic acid, furan-2-carboxylic acid, indole-2-carboxylic acid, indole-3-carboxylic acid, *N*-Boc-L-proline or *N*-Boc-D-proline) afforded Boc-protected derivatives **7a**, **7b**, **9**, **11**, **12a**, **12b**, **14** and **16a–c** which were converted into final compounds upon cleavage of the Boc protecting group with either gaseous hydrochloric acid or acetyl chloride–ethanol as a convenient reagent for *in situ* HCl formation [37].

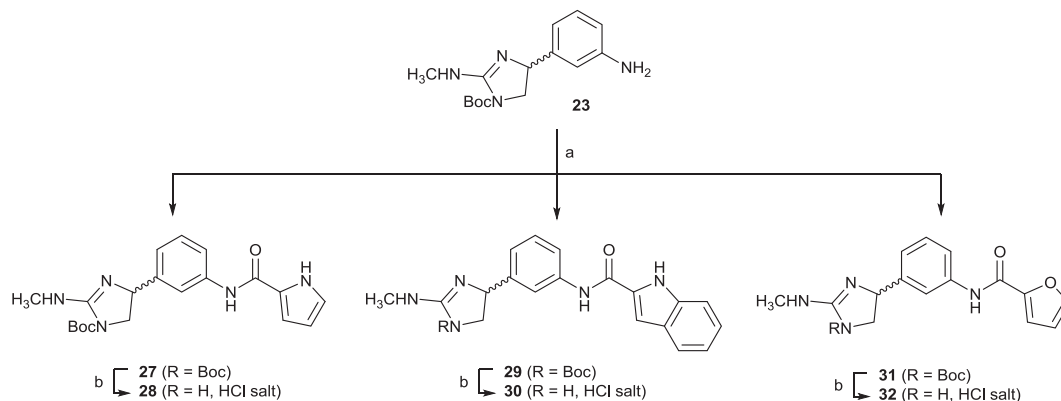
N-Methylated intermediates **22** and **23** were prepared according to Scheme 3. 2-(*N*-Methylamino)-pyrimidine (**18**) was prepared by heating 2-aminopyrimidine and iodomethane in acetone followed by treatment with 10% aqueous sodium hydroxide. This was then reacted with 2-bromo-3-nitroacetophenone in acetonitrile and a catalytic amount of 4-dimethylaminopyridine to afford 2-hydroxy-

1-methyl-2-(3-nitrophenyl)-2,3-dihydro-1*H*-imidazo[1,2-*a*]pyrimidin-4-ium bromide (**19**). After hydrazinolysis in ethanol using microwave irradiation and subsequent Dimroth-type rearrangement, compound **19** was converted into 2-(*N*-methylamino)-imidazole **20** [36]. Boc protection of the imidazole *N*-1 of compound **20**, followed by reduction of the nitro group afforded the amine **22**. A prolonged catalytic hydrogenation (24 h) enabled both, the reduction of the nitro group and the imidazole $\text{C}=\text{C}$ bond, to give the 4,5-dihydro-2-(*N*-methylamino)-imidazole derivative **23**.

4-Phenyl-2-(*N*-methylamino)-imidazoles **24–26**, and 4-phenyl-4,5-dihydro-2-(*N*-methylamino)-imidazoles **27–32** were prepared according to Schemes 4 and 5. TBTU-promoted coupling of amines **22** or **23**, and the corresponding carboxylic acid (pyrrole-2-



Scheme 4. Synthesis of 4-phenyl-2-(*N*-methylamino)-imidazoles **24–26**. *Reagents and conditions:* (a) corresponding carboxylic acid, TBTU, NMM, CH_2Cl_2 , 35°C , 24 h; (b) $\text{HCl}_{(\text{g})}$, THF/ EtOH , rt, 5 h.



Scheme 5. Synthesis of 4-phenyl-4,5-dihydro-(*N*-methylamino)-imidazoles **27–32**. *Reagents and conditions:* (a) corresponding carboxylic acid, TBTU, NMM, CH_2Cl_2 , 35°C , 24 h; (b) $\text{HCl}_{(\text{g})}$, EtOH , rt, 5 h.

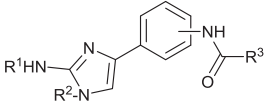
carboxylic acid, indole-2-carboxylic acid or furan-2-carboxylic acid) afforded Boc-protected derivatives **24**, **25**, **27**, **29** and **31** which were converted into end products upon cleavage of the Boc protecting group.

2.2. Biological evaluation

In total, twenty eight novel compounds were synthesized and studied for their ability to block the human sodium channel isoforms Na_v1.3, Na_v1.4 and Na_v1.5, as well as their selectivity against the human cardiac isoform Na_v1.7. The screening was performed using an automated patch clamp electrophysiology assay on the Sophion QPatch HT system (Sophion Bioscience A/S). Compounds of three different structural classes, (i) 4-phenyl-2-aminoimidazoles **6–17**, (ii) 4-phenyl-2-(*N*-methylamino)-imidazoles **24–26**, and (iii) 4-phenyl-4,5-dihydro-2-(*N*-methylamino)-imidazoles **27–32**, were tested and their IC₅₀ values, i.e. concentrations of compounds that inhibit sodium channel currents by 50%, are presented in Tables 1 and 2. The IC₅₀ values of synthesized compounds against each Na_v isoforms were determined from concentration–response relationships established by cumulatively applying four escalating concentrations (0.3–10 μM) of test compound to a cell, as detailed in the Experimental section. All of the active compounds acted as state-dependent VGSC modulators, blocking only the open-inactivated state of the channels (depolarization from ~−70 mV) and possessing no activity on the closed state of the channels, with IC₅₀ values higher than 30 μM (depolarization from −100 mV, data

Table 1

Modulatory activities of 4-phenyl-2-aminoimidazoles **6–17** and 4-phenyl-2-(*N*-methylamino)-imidazoles **24–26** on the open-inactivated state of the Na_v channel isoforms.



Compd	R ¹	R ²	R ³	Subst	IC ₅₀ (μM) ^a	Na _v channel isoforms			
						Na _v 1.3	Na _v 1.4	Na _v 1.5	Na _v 1.7
6	H	Pyrrol-2-yl	Pyrrol-2-yl	1,3	25	— ^b	27	19	
7a	H	Boc	Pyrrol-2-yl	1,3	25	25	— ^b	— ^b	
7b	H	Boc	Pyrrol-2-yl	1,4	— ^b	— ^b	— ^b	— ^b	
8a^c	H	H	Pyrrol-2-yl	1,3	— ^b	— ^b	— ^b	— ^b	
8b^c	H	H	Pyrrol-2-yl	1,4	— ^b	— ^b	— ^b	— ^b	
9	H	Boc	Pyrrol-3-yl	1,3	23	— ^b	— ^b	— ^b	
10^c	H	H	Pyrrol-3-yl	1,3	12	15	— ^b	— ^b	
11	H	Boc	Furan-2-yl	1,4	27	— ^b	— ^b	22	
12a	H	Boc	Indol-2-yl	1,3	26	— ^b	— ^b	— ^b	
12b	H	Boc	Indol-2-yl	1,4	22	28	— ^b	— ^b	
13a^c	H	H	Indol-2-yl	1,3	— ^b	— ^b	— ^b	— ^b	
13b^c	H	H	Indol-2-yl	1,4	— ^b	— ^b	— ^b	— ^b	
14	H	Boc	Indol-3-yl	1,3	27	26	— ^b	— ^b	
15^c	H	H	Indol-3-yl	1,3	12	14	— ^b	26	
16a	H	Boc	(<i>R</i>)-Pyrrolidin-2-yl	1,3	— ^b	— ^b	— ^b	29	
16b	H	Boc	(<i>R</i>)-Pyrrolidin-2-yl	1,4	— ^b	— ^b	20	— ^b	
16c	H	Boc	(<i>S</i>)-Pyrrolidin-2-yl	1,4	25	— ^b	— ^b	19	
17a^c	H	H	(<i>R</i>)-Pyrrolidin-2-yl	1,3	8	— ^b	— ^b	28	
17b^c	H	H	(<i>S</i>)-Pyrrolidin-2-yl	1,4	13	— ^b	— ^b	— ^b	
24	CH ₃	Boc	Furan-2-yl	1,3	— ^b	— ^b	— ^b	26	
25	CH ₃	Boc	Indol-2-yl	1,3	— ^b	— ^b	— ^b	— ^b	
26^c	CH ₃	H	Indol-2-yl	1,3	— ^b	— ^b	20	— ^b	
Lidocaine					10.5	2	N/A ^d	29	

^a The concentration of compound that inhibits a sodium channel current by 50%. Each IC₅₀ value is the mean of three independent experiments.

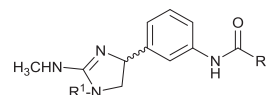
^b IC₅₀ value higher than 30 μM.

^c HCl salt.

^d N/A: not available.

Table 2

Modulatory activities of 4-phenyl-4,5-dihydro-2-(*N*-methylamino)-imidazoles **27–32** on the open-inactivated state of the Na_v channel isoforms.



Compd	R ¹	R ²	IC ₅₀ (μM) ^a			
			Na _v 1.3	Na _v 1.4	Na _v 1.5	Na _v 1.7
27	Boc	Pyrrol-2-yl	24	— ^b	24	23
28^c	H	Pyrrol-2-yl	21	— ^b	— ^b	26
29	Boc	Indol-2-yl	— ^b	— ^b	3	18
30^c	H	Indol-2-yl	— ^b	— ^b	— ^b	— ^b
31	Boc	Furan-2-yl	— ^b	— ^b	— ^b	— ^b
32^c	H	Furan-2-yl	22	— ^b	— ^b	27
Lidocaine			10.5	2	N/A ^d	29

^a The concentration of compound that inhibits a sodium channel current by 50%.

Each IC₅₀ value is the mean of three independent experiments.

^b IC₅₀ value higher than 30 μM.

^c HCl salt.

^d N/A: not available.

not shown). IC₅₀ values for lidocaine as reference substance were 10.5 μM against Na_v1.3, 2.1 μM against Na_v1.4 and 29 μM against Na_v1.7 channel. Activity of lidocaine against Na_v1.5 isoform was not determined.

Several compounds exhibited promising activities on different Na_v channel isoforms in medium micromolar range and some of the compounds showed also moderate isoform selectivities, e.g., compounds **8b**, **9**, **12a**, **16a**, **16b**, **17b**, **24** and **26**. The most promising results were obtained for the Na_v1.3 channel where four compounds had IC₅₀ values lower than 15 μM. The most potent compound was the (*R*)-proline derivative **17a** blocking Na_v1.3 with an IC₅₀ value of 8 μM. Compound **17a** was selective towards Na_v1.4 and Na_v1.5, and weakly active against the Na_v1.7 isoform (IC₅₀ = 28 μM). Channel-blocking activity against the Na_v1.3 with an IC₅₀ value of 13 μM was observed also for compound **17b**, an (*S*)-proline-containing analog of **17a** with a 1,4-substitution pattern on the phenyl ring. Moreover, compound **17b** did not possess any activity on other isoforms and could thus represent a starting point for the development of selective modulators of Na_v1.3. Two other compounds of the series, pyrrol-3-yl derivative **10** and indol-3-yl derivative **15**, also possessed Na_v1.3 modulatory activity, both with an IC₅₀ value of 12 μM. Both compounds were also active against the Na_v1.4 isoform with IC₅₀ values of 15 μM and 14 μM, respectively. Interestingly, isomers of compounds **10** and **15** containing 2- instead of 3-substituted pyrrole or indole rings, pyrrol-2-yl derivative **8a** and indol-2-yl derivative **13a** were devoid of activity on all Na_v channel isoforms, suggesting the importance of the orientation of pyrrole or indole rings for antagonist activity. Furthermore, based on comparison of the isomeric pyrrol-3-yl derivatives **7a** (IC₅₀ value of 25 μM against Na_v1.3) and **7b** (IC₅₀ value >30 μM against Na_v1.3), the 1,3-substitution pattern on the phenyl ring is preferred over 1,4-substitution pattern for the Na_v1.3 modulatory activity.

The most active modulators of the skeletal muscle isoform Na_v1.4 were 4-phenyl-2-aminoimidazoles **10** (IC₅₀ = 15 μM) and **15** (IC₅₀ = 14 μM) which were also active against the Na_v1.3 channel with IC₅₀ values of 12 μM. The introduction of *N*-methyl substituent on the primary amino group of 2-aminoimidazole ring in derivatives **24–32** resulted in complete loss of activity against the Na_v1.4 isoform.

The Na_v1.5 channel isoform is located in the heart. Blockade of this channel is associated with increased risk of a cardiac side-effect

liability, and it is regarded as an unwanted activity in any therapeutic molecule. Fortunately, the majority of tested compounds were almost inactive against the Nav1.5, with the exception of compound **29** with an IC₅₀ of 3 μ M.

The Nav1.7 isoform is mainly located in the peripheral nervous system and has been identified as a promising drug target for the treatment of neuropathic pain [15]. The most active compound against the Nav1.7 channel was the indol-2-yl derivative **29** (IC₅₀ = 18 μ M), but as it also displayed activity against the Nav1.5 isoform (IC₅₀ = 3 μ M) it is not suitable for further development. A moderate activity against the Nav1.7 isoform was observed also for 4-phenyl-2-aminoimidazoles **6** and **16c**, both having IC₅₀ values of 19 μ M. Compound **16c** displayed also a weak Nav1.3 modulatory activity with IC₅₀ value of 25 μ M. As both, Nav1.3 and Nav1.7 channels have been linked to nociceptive processing, finding compounds of dual activity against both isoforms could lead to synergistic effects and contribute to favorable therapeutic profiles of such compounds. Interestingly, compound **16b**, the *R* isomer of **16c**, was not active neither against the Nav1.3 nor the Nav1.7 channels.

3. Conclusion

We have designed and synthesized a series of clathrocin analogs and evaluated their effects on human Nav1.3–1.5 and Nav1.7 channels using an automated patch clamp electrophysiology assay. Several compounds exhibited promising activities with moderate isoform selectivities. All of the active compounds acted as state-dependent VGSC modulators. The most promising results were obtained for the Nav1.3 channel, against which four compounds were found to possess IC₅₀ values lower than 15 μ M. The results provide valuable information on structure–activity relationships and offer good prospect for the development of isoform selective VGSC modulators.

4. Experimental section

4.1. Electrophysiology

Cells were prepared by dissociation from T175 cell culture flasks using trypsin–EDTA (0.05%), cells were kept in serum free media in the cell hotel on board the QPatch HT. These cells were sampled, washed and re-suspended in extracellular recording solution by the QPatch HT immediately before application to well site on the chip. Once in whole-cell configuration, vehicle (0.1% DMSO v/v) was applied to the cells to achieve a stable control recording (4-min total). This was followed by application of test concentrations as a single bolus addition (4-min incubation per test concentration). Compounds were prepared in extracellular recording solution from a 10 mM (100% DMSO) stock to yield a final 10 μ M (0.1% DMSO) test concentration from which subsequent serial dilutions in extracellular solution were performed (0.3–10 μ M). Voltage protocols for the sodium channels being screened were designed to reflect the high-frequency, pathophysiological state of the channels that may be therapeutic targets (Nav1.3, Nav1.4 and Nav1.7), and the low-frequency, physiological state of the safety target (Nav1.5). Currents were elicited from Nav1.3, Nav1.4 and Nav1.7 cell lines using a standard two-pulse voltage protocol. From a holding potential of –100 mV, a 20 ms activating step to –20 mV was applied to assess the effect of compounds on resting (closed) state block. The second activating pulse was applied following a 5-s pre-pulse to half inactivation potential (variable depending on the sodium channel studied, –65 to –75 mV) to assess block on the open-inactivated state of the channel. This protocol was applied at a sweep interval of 0.067 Hz throughout the duration of the

experiment. To study Nav1.5 currents, a pulse train consisting of 10 repetitive activating test pulses to –20 mV from a holding potential of –100 mV were applied at a 1 Hz frequency until 10 pulses were reached, this sequence was repeated at a sweep interval of 0.016 Hz throughout the duration of the experiment. For Nav1.3, Nav1.4 and Nav1.7 channels the peak inward current was determined for both the closed and open-inactivated test pulses from each sweep applied to the cells and for Nav1.5 from the tenth pulse of each pulse train recorded. Data was captured using QPatch assay software (v5.0). The % inhibition of peak current was calculated as the mean peak current value for the last three sweeps measured in each concentration test period relative to the last three sweeps recorded during the control vehicle period. Sigmoidal concentration response curves (four parameter logistic curves) were fitted to the % inhibition data using Xlfit (IDBS) from which the IC₅₀ was determined. Fits were constrained at 0 and 100%. Data are presented as mean \pm SD for minimum of 3 independent observations.

4.2. Chemistry – general

Chemicals were obtained from Acros, Aldrich Chemical Co., and Fluka and used without further purification. Analytical TLC was performed on silica gel Merck 60 F₂₅₄ plates (0.25 mm), using visualization with UV light and ninhydrin. Column chromatography was carried out on silica gel 60 (particle size 240–400 mesh). HPLC analyses were performed on an Agilent Technologies 1100 instrument with a G1365B UV-VIS detector, a G1316A thermostat and a G1313A autosampler using a Phenomenex Luna 5 μ m C18 column (4.6 \times 150 mm or 4.6 \times 250 mm) and flow rate of 1.0 mL/min. The eluent consisted of trifluoroacetic acid (0.1% in water) or ammonia (0.1% in water) as solvent A and methanol as solvent B. Microwave-assisted reactions were performed using a CEM Discover microwave reactor (CEM Corp.). Melting points were determined on a Reichert hot stage microscope and are uncorrected. ¹H NMR and ¹³C NMR spectra were recorded at 400 and 100 MHz, respectively, on a Bruker AVANCE III 400 spectrometer in DMSO-*d*₆ or MeOH-*d*₄ solution, with TMS as the internal standard. IR spectra were recorded on a Perkin–Elmer Spectrum BX FT-IR spectrometer or Thermo Nicolet Nexus 470 ESP FT-IR spectrometer. Mass spectra were obtained using a VGAnalytical Autospec Q mass spectrometer. Optical rotations were measured on a Perkin–Elmer 241 MC polarimeter. The reported values for specific rotation are average values of 10 successive measurements using an integration time of 5 s. The purity of the tested compounds was established to be \geq 95%.

4.3. Synthetic procedures

4.3.1. General procedure A. Synthesis of compounds **1a–c** (with **1c** as an example)

To a solution of 2-aminopyrimidine (325 mg, 3.41 mmol) and 2-bromo-4-nitroacetophenone (1.00 g, 4.10 mmol) in acetonitrile (15 mL) 4-dimethylaminopyridine (4.2 mg, 0.034 mmol) was added. After being stirred at 85 °C for 5 h, the reaction mixture was filtered, washed with acetonitrile (10 mL) and ether (2 \times 10 mL), and dried to give **1c**.

4.3.1.1. 2-(3-Nitrophenyl)-1H-imidazo[1,2-a]pyrimidin-4-ium bromide (1c**).** Yield, 66% (0.726 g); orange solid; mp 251–255 °C; IR (KBr) ν = 3075, 3023, 2674, 2579, 2557, 1642, 1526, 1483, 1341, 1304, 1234, 1109, 1083, 928, 915, 805, 790, 732 cm^{–1}. ¹H NMR (DMSO-*d*₆) δ 7.41 (dd, 1H, ³J₁ = 6.8 Hz, ³J₂ = 4.4 Hz, Ar-H-6), 7.86 (t, 1H, ³J = 8.0 Hz, Ar-H-5'), 8.29–8.32 (m, 1H, Ar-H-4'/6'), 8.45–8.48 (m, 1H, Ar-H-4'/6'), 8.83–8.85 (m, 2H, Ar-H-3, Ar-H-7), 8.86 (t, 1H, ⁴J = 2.0 Hz, Ar-H-2'), 9.20 (dd, 1H, ³J = 6.8 Hz, ⁴J = 2.0 Hz, Ar-H-5), signal for the NH proton not seen; ¹³C NMR (DMSO-*d*₆) δ 110.46,

112.40, 120.53, 124.14, 130.71, 130.94, 132.20, 137.08, 137.18, 145.82, 148.45, 155.45; MS (ESI) m/z (%) = 241 ([M – Br]⁺, 100). HRMS for C₁₂H₉N₄O₂: calculated 241.0726; found 241.0724.

4.3.2. General procedure B. Synthesis of compounds **2a** and **2b** (with **2a** as an example)

To a suspension of **1a** or **1c** (0.590 mmol) in ethanol (3 mL) in a 10 mL glass vessel hydrazine hydrate (0.369 mL, 35% hydrazine in solution, 4.13 mmol) was added, the vessel was sealed, placed in a microwave reactor, and heated at 120 °C for 40 min (maximum power = 50 W, ramp time = 3 min). The mixture was cooled to rt, the solvent evaporated and the resulting residue was purified by flash column chromatography using dichloromethane/methanol = 10/1 with dissolved NH_{3(g)} as an eluent, to afford 2-aminoimidazole **2a**.

4.3.2.1. 4-(3-Nitrophenyl)-1H-imidazol-2-amine (2a). Yield, 90%; orange solid; mp 180–182 °C; IR (KBr) ν = 3446, 3361, 3079, 2854, 2674, 1622, 1548, 1516, 1482, 1342, 1260, 1173, 1146, 1033, 867, 799, 725 cm⁻¹. ¹H NMR (DMSO-*d*₆) δ 5.45 (s, 2H, NH₂, D₂O exchangeable), 7.27 (s, 1H, Ar-H-5), 7.55 (t, 1H, ³J = 8.0 Hz, Ar-H-5'), 7.90–7.93 (m, 1H, Ar-H-4'/6'), 8.01–8.04 (m, 1H, Ar-H-4'/6'), 8.42 (s, 1H, Ar-H-2'), 10.59 (br s, 1H, NH, D₂O exchangeable); ¹³C NMR (MeOH-*d*₄) δ 111.54, 117.78, 119.72, 129.24, 129.29, 132.87, 135.84, 148.76, 151.14; MS (ESI) m/z (%) = 205 (MH⁺, 100). HRMS for C₉H₉N₄O₂: calculated 205.0726; found 205.0721.

4.3.3. General procedure C. Synthesis of compounds **3a** and **3b** (with **3a** as an example)

To a suspension of **2a** (0.500 g, 2.45 mmol) in a mixture of methanol (10 mL) and water (5 mL) Boc-anhydride (1.07 g, 2.90 mmol) was added and the mixture was stirred at rt for 3 h. The precipitate was filtered off, washed with methanol (2 × 5 mL) and dried to give **3a**.

4.3.3.1. tert-Butyl 2-amino-4-(3-nitrophenyl)-1H-imidazole-1-carboxylate (3a). Yield, 95%; yellow solid; mp 178–180 °C; IR (KBr) ν = 3413, 3278, 3122, 2982, 1739, 1637, 1526, 1477, 1447, 1344, 1320, 1273, 1257, 1212, 1152, 1119, 1066, 903, 836, 773, 716 cm⁻¹. ¹H NMR (DMSO-*d*₆) δ 1.60 (s, 9H, *t*-Bu), 6.73 (br s, 2H, NH₂, D₂O exchangeable), 7.64 (t, 1H, ³J = 8.0 Hz, Ar-H-5'), 7.67 (s, 1H, Ar-H-5), 8.06–8.09 (m, 1H, Ar-H-4'/6'), 8.19–8.22 (m, 1H, Ar-H-4'/6'), 8.55 (t, 1H, ⁴J = 2.0 Hz, Ar-H-2'); ¹³C NMR (DMSO-*d*₆) δ 28.00 (CCH₃), 85.45 (CCH₃), 108.88, 119.33, 121.80, 130.40, 131.31, 135.28, 135.78, 148.70, 149.25, 151.18; MS (ESI) m/z (%) = 305 (MH⁺, 10), 249 ([MH – *t*-Bu]⁺, 90), 205 ([MH – Boc]⁺, 100). HRMS for C₁₄H₁₇N₄O₄: calculated 305.1250; found 305.1255.

4.3.4. General procedure D. Synthesis of compounds **4a**, **4b** and **5** (with **4a** as an example)

Compound **3a** (1.00 g, 3.29 mmol) was dissolved in THF (50 mL), Pd/C (200 mg) was added and the reaction mixture was stirred under hydrogen atmosphere for 5 h. The catalyst was filtered off and the solvent removed under reduced pressure to give **4a**.

4.3.4.1. tert-Butyl 2-amino-4-(3-aminophenyl)-1H-imidazole-1-carboxylate (4a). Yield, 95%; white solid; mp 160–162 °C; IR (KBr) ν = 3424, 3345, 3127, 2972, 1737, 1636, 1617, 1546, 1452, 1359, 1326, 1267, 1239, 1207, 1159, 1119, 1062, 847, 769, 721 cm⁻¹. ¹H NMR (DMSO-*d*₆) δ 1.58 (s, 9H, *t*-Bu), 5.02 (br s, 2H, NH₂, D₂O exchangeable), 6.42–6.45 (m, 1H, Ar-H-4'/6'), 6.55 (br s, 2H, NH₂, D₂O exchangeable), 6.86–6.88 (m, 1H, Ar-H-4'/6'), 6.95–6.99 (m, 2H, Ar-H-2', Ar-H-5'), 7.12 (s, 1H, Ar-H-5); ¹³C NMR (DMSO-*d*₆) δ 27.50 (CCH₃), 84.48 (CCH₃), 105.28, 110.32, 112.60, 112.80, 128.76, 133.78,

137.69, 148.57, 148.91, 150.15; MS (ESI) m/z (%) = 275 (MH⁺, 100). HRMS for C₁₄H₁₉N₄O₂: calculated 275.1508; found 275.1504.

4.3.5. General procedure E. Synthesis of compounds **7a**, **7b**, **9**, **11**, **12a**, **12b**, **14**, **16a–c**, **24**, **25**, **27**, **29** and **31** (with **7a** as an example)

To a suspension of pyrrole-2-carboxylic acid (122 mg, 1.09 mmol) and TBTU (380 mg, 1.18 mmol) in dichloromethane (5 mL) *N*-methylmorpholine (0.501 mL, 4.56 mmol) was added, and the mixture stirred at rt for 0.5 h upon which a clear solution formed. Compound **4a** (250 mg, 0.91 mmol) was added and the mixture stirred at 35 °C overnight. The solvent was evaporated in vacuo, the residue dissolved in ethyl acetate (30 mL), and washed successively with water (2 × 10 mL), saturated aqueous NaHCO₃ solution (2 × 10 mL), and brine (1 × 10 mL). The organic phase was dried over Na₂SO₄, filtered and the solvent evaporated under reduced pressure. The crude product was purified by flash column chromatography using ethyl acetate/petroleum ether or dichloromethane/methanol as an eluent, to afford **7a**.

4.3.5.1. tert-Butyl 4-(3-(1H-pyrrole-2-carboxamido)phenyl)-2-amino-1H-imidazole-1-carboxylate (7a). Yield, 45% (150 mg); white solid; mp 175–177 °C; IR (KBr) ν = 3404, 3354, 3142, 2976, 1731, 1644, 1555, 1517, 1431, 1361, 1311, 1255, 1199, 1157, 1122, 1089, 1038, 758, 716 cm⁻¹. ¹H NMR (DMSO-*d*₆) δ 1.59 (s, 9H, *t*-Bu), 6.16–6.18 (m, 1H, Pyr-H), 6.63 (br s, 2H, NH₂, D₂O exchangeable), 6.96–6.98 (m, 1H, Pyr-H), 7.09–7.11 (m, 1H, Pyr-H), 7.26 (s, 1H, Ar-H-5), 7.29 (t, 1H, ³J = 8.0 Hz, Ar-H-5'), 7.41–7.43 (m, 1H, Ar-H-4'/6'), 7.67–7.69 (m, 1H, Ar-H-4'/6'), 8.07 (t, 1H, ⁴J = 2.0 Hz, Ar-H-2'), 9.77 (s, 1H, NH, D₂O exchangeable), 11.63 (s, 1H, NH, D₂O exchangeable); ¹³C NMR (DMSO-*d*₆) δ 27.51 (CCH₃), 84.67 (CCH₃), 105.93, 108.89, 111.25, 116.28, 118.54, 119.41, 122.47, 126.06, 128.57, 133.69, 137.03, 139.47, 148.88, 150.39, 159.08; MS (ESI) m/z (%) = 368 (MH⁺, 20), 312 ([MH – *t*-Bu]⁺, 100), 268 ([MH – Boc]⁺, 60). HRMS for C₁₉H₂₂N₅O₃: calculated 368.1723; found 368.1724. HPLC: Phenomenex Luna 5 μ m C18 column (4.6 mm × 150 mm); mobile phase: 30–80% of MeOH in TFA (0.1%) in 25 min; flow rate 1.0 mL/min; injection volume: 20 μ L; retention time: 9.813 min (99.6% at 254 nm, 99.3% at 280 nm).

4.3.6. General procedure F. Synthesis of compounds **8a**, **10**, **13a**, **15**, **17a**, **26**, **28**, **30** and **32** (with **8a** as an example)

Solution of compound **7a** (108 mg, 0.250 mmol) in a 1:1 mixture of THF and EtOH (15 mL) was saturated with gaseous HCl and stirred at rt for 5 h. The solvent was removed under reduced pressure, the solid was filtered off and washed with diethyl ether (3 × 5 mL), to afford **8a**.

4.3.6.1. 4-(3-(1H-Pyrrole-2-carboxamido)phenyl)-2-amino-1H-imidazol-3-ium chloride (8a). Yield, 85% (76 mg); brown foam; mp 170–174 °C; IR (KBr) ν = 3232, 3142, 2972, 2766, 1676, 1625, 1607, 1547, 1529, 1486, 1422, 1324, 1227, 1158, 1114, 1044, 883, 742 cm⁻¹. ¹H NMR (DMSO-*d*₆) δ 6.17–6.19 (m, 1H, Pyr-H), 6.97–6.99 (m, 1H, Pyr-H), 7.09–7.11 (m, 1H, Pyr-H), 7.28 (s, 1H, Ar-H-5), 7.34 (d, 1H, ³J = 8.0 Hz, Ar-H-4'/6'), 7.41 (t, 1H, ³J = 8.0 Hz, Ar-H-5'), 7.48 (s, 2H, NH₂, D₂O exchangeable), 7.67 (d, 1H, ³J = 8.0 Hz, Ar-H-4'/6'), 8.03 (s, 1H, Ar-H-2'), 10.04 (s, 1H, NH, D₂O exchangeable), 11.80 (s, 1H, NH, D₂O exchangeable), 12.18 (br s, 1H, NH, D₂O exchangeable), 12.87 (br s, 1H, NH, D₂O exchangeable); ¹³C NMR (DMSO-*d*₆) δ 108.95, 109.32, 111.86, 116.11, 119.22, 120.00, 122.65, 125.86, 126.48, 128.01, 129.20, 139.83, 147.77, 159.12; MS (ESI) m/z (%) = 268 ([M – Cl]⁺, 100). HRMS for C₁₄H₁₄N₅O: calculated 268.1198; found 268.1193. HPLC: Phenomenex Luna 5 μ m C18 column (4.6 mm × 150 mm); mobile phase: 10–90% of MeOH in TFA (0.1%) in 20 min; flow rate 1.0 mL/min; injection volume: 20 μ L; retention time: 13.386 min (95.1% at 254 nm, 95.1% at 280 nm).

4.3.7. General procedure G. Synthesis of compounds **8b**, **13b** and **17b** (with **8b** as an example)

To an ice cold solution of **7b** (200 mg, 0.544 mmol) in ethanol (4 mL) acetyl chloride (600 μ L, 8.4 mmol) was added dropwise. After being stirred at 0 °C for 1 h the reaction mixture was allowed to warm to rt, the solvent and the excess HCl were evaporated and the solid residue was triturated with diethyl ether, yielding **8b**.

4.3.7.1. 4-(4-(1H-Pyrrole-2-carboxamido)phenyl)-2-amino-1H-imidazol-3-ium chloride (8b**).** Yield, 42% (69 mg); white solid; mp 114–116 °C; IR (KBr) ν = 3421, 1656, 1412, 1333, 1124, 836, 746 cm^{-1} . ^1H NMR (DMSO- d_6) δ 6.16–6.19 (m, 1H, Pyrr-H), 6.98 (br s, 2H, NH₂, D₂O exchangeable), 7.08 (s, 1H, Pyrr-H), 7.29 (s, 1H, Pyrr-H), 7.41 (s, 1H, Ar-H-5), 7.61 (d, 2H, 3J = 8.7 Hz, Ar-H-2',6'/3',5'), 7.84 (d, 2H, 3J = 8.7 Hz, Ar-H-2',6'/3',5'), 9.94 (s, 1H, NH, D₂O exchangeable), 11.73 (s, 1H, NH, D₂O exchangeable), 12.02 (s, 1H, NH, D₂O exchangeable), 12.76 (s, 1H, NH, D₂O exchangeable); ^{13}C NMR (DMSO- d_6) δ 108.44, 108.96, 111.73, 119.88, 122.24, 122.73, 124.60, 125.89, 126.45, 139.20, 147.46, 159.08; MS (ESI) m/z = 268 [M – Cl]⁺. HRMS for C₁₄H₁₄N₅O: calculated 268.1198; found 268.1194. HPLC: Phenomenex Luna 5 μ m C18 column (4.6 mm \times 150 mm); mobile phase: 50–80% of methanol in trifluoroacetic acid (0.1%) in 30 min; flow rate 1.0 mL/min; injection volume: 10 μ L; retention time: 12.880 min (95.1% at 254 nm).

Acknowledgment

This work was supported by the Slovenian Research Agency (grant no. P1-0208 and grant no. Z1-5458) and by the EU FP7 Integrated Project MAREX (project no. FP7-KBBE-2009-3-245137). We thank the Biology Department at Xention for the contributions to this project.

Appendix A. Supplementary data

Supplementary data related to this article can be found at <http://dx.doi.org/10.1016/j.ejmech.2013.12.034>.

References

- [1] J. Payandeh, T.M.G. El-Din, T. Scheuer, N. Zheng, W.A. Catterall, Crystal structure of a voltage-gated sodium channel in two potentially inactivated states, *Nature* 486 (2012) 135–139.
- [2] X. Zhang, W.L. Ren, P. DeCaen, C.Y. Yan, X. Tao, L. Tang, J.J. Wang, K. Hasegawa, T. Kumasaka, J.H. He, J.W. Wang, D.E. Clapham, N. Yan, Crystal structure of an orthologue of the NaChBac voltage-gated sodium channel, *Nature* 486 (2012) 130–134.
- [3] J. Payandeh, T. Scheuer, N. Zheng, W.A. Catterall, The crystal structure of a voltage-gated sodium channel, *Nature* 475 (2011) 353–358.
- [4] W.A. Catterall, Ion channel voltage sensors: structure, function, and pathophysiology, *Neuron* 67 (2010) 915–928.
- [5] F.H. Yu, W.A. Catterall, Overview of the voltage-gated sodium channel family, *Genome Biol.* 4 (2003).
- [6] C. Sato, Y. Ueno, K. Asai, K. Takahashi, M. Sato, A. Engel, Y. Fujiyoshi, The voltage-sensitive sodium channel is a bell-shaped molecule with several cavities, *Nature* 409 (2001) 1047–1051.
- [7] W.A. Catterall, From ionic currents to molecular mechanisms: the structure and function of voltage-gated sodium channels, *Neuron* 26 (2000) 13–25.
- [8] V. Zuliani, M.K. Patel, M. Fantini, M. Rivara, Recent advances in the medicinal chemistry of sodium channel blockers and their therapeutic potential, *Curr. Top. Med. Chem.* 9 (2009) 396–415.
- [9] S. England, M.J. de Groot, Subtype-selective targeting of voltage-gated sodium channels, *Br. J. Pharmacol.* 158 (2009) 1413–1425.
- [10] I. Tarnawa, H. Bolcskei, P. Kocsis, Blockers of voltage-gated sodium channels for the treatment of central nervous system diseases, *Recent Pat. CNS Drug Discov.* 2 (2007) 57–78.
- [11] J.N. Wood, J. Boorman, Voltage-gated sodium channel blockers; target validation and therapeutic potential, *Curr. Top. Med. Chem.* 5 (2005) 529–537.
- [12] D.S. Ragsdale, How do mutant Nav1.1 sodium channels cause epilepsy? *Brain Res. Rev.* 58 (2008) 149–159.
- [13] C. Lossin, T.H. Rhodes, R.R. Desai, C.G. Vanoye, D. Wang, S. Carniciu, O. Devinsky, A.L. George, Epilepsy-associated dysfunction in the voltage-gated neuronal sodium channel SCN1A, *J. Neurosci.* 23 (2003) 11289–11295.
- [14] K.M. Kahlig, T.H. Rhodes, M. Pusch, T. Freilinger, J.M. Pereira-Monteiro, M.D. Ferrari, A.M.J.M. van den Maagdenberg, M. Dichgans, A.L. George, Divergent sodium channel defects in familial hemiplegic migraine, *Proc. Natl. Acad. Sci. U. S. A.* 105 (2008) 9799–9804.
- [15] S.B. Hoyt, C. London, C. Abbadié, J.P. Felix, M.L. Garcia, N. Jochnowitz, B.V. Karanam, X.H. Li, K.A. Lyons, E. McGowan, B.T. Priest, M.M. Smith, V.A. Warren, B.S. Thomas-Fowlkes, G.J. Kaczorowski, J.L. Duffy, A novel benzazepinone sodium channel blocker with oral efficacy in a rat model of neuropathic pain, *Bioorg. Med. Chem. Lett.* 23 (2013) 3640–3645.
- [16] S.D. Dib-Hajj, A.M. Binshtok, T.R. Cummins, M.F. Jarvis, T. Samad, K. Zimmermann, Voltage-gated sodium channels in pain states: role in pathophysiology and targets for treatment, *Brain Res. Rev.* 60 (2009) 65–83.
- [17] S.C. Cannon, Spectrum of sodium channel disturbances in the nondystrophic myotonias and periodic paralyses, *Kidney Int.* 57 (2000) 772–779.
- [18] T. Zimmer, R. Surber, SCN5A channelopathies – an update on mutations and mechanisms, *Prog. Biophys. Mol. Biol.* 98 (2008) 120–136.
- [19] A. Wickenden, B. Priest, G. Erdemli, Ion channel drug discovery: challenges and future directions, *Future Med. Chem.* 4 (2012) 661–679.
- [20] J.J. Clare, S.N. Tate, M. Nobbs, M.A. Romanos, Voltage-gated sodium channels as therapeutic targets, *Drug. Discov. Today* 5 (2000) 506–520.
- [21] H.N. Nguyen, H. Bregman, J.L. Buchanan, B.F. Du, E. Feric, L.Y. Huang, X.W. Li, J. Ligutti, D. Liu, A.B. Malmberg, D.J. Matson, J.S. McDermott, V.F. Patel, B. Wilenkin, A.R. Zou, S.I. McDonough, E.F. DiMauro, Discovery and optimization of aminopyrimidinones as potent and state-dependent Nav1.7 antagonists, *Bioorg. Med. Chem. Lett.* 22 (2012) 1055–1060.
- [22] N. Chakka, H. Bregman, B.F. Du, H.N. Nguyen, J.L. Buchanan, E. Feric, J. Ligutti, D. Liu, J.S. McDermott, A.R. Zou, S.I. McDonough, E.F. DiMauro, Discovery and hit-to-lead optimization of pyrrolopyrimidines as potent, state-dependent Nav1.7 antagonists, *Bioorg. Med. Chem. Lett.* 22 (2012) 2052–2062.
- [23] H. Bregman, H.N. Nguyen, E. Feric, J. Ligutti, D. Liu, J.S. McDermott, B. Wilenkin, A.R. Zou, L.Y. Huang, X.W. Li, S.I. McDonough, E.F. DiMauro, The discovery of aminopyrazines as novel, potent Nav1.7 antagonists: hit-to-lead identification and SAR, *Bioorg. Med. Chem. Lett.* 22 (2012) 2033–2042.
- [24] I. Macsari, L. Sandberg, Y. Besidski, Y. Gravenfors, T. Gimnani, J. Bylund, T. Bueters, A.B. Eriksson, P.E. Lund, E. Venyike, P.I. Arvidsson, Phenyl isoxazole voltage-gated sodium channel blockers: structure and activity relationship, *Bioorg. Med. Chem. Lett.* 21 (2011) 3871–3876.
- [25] H. Bregman, L. Berry, J.L. Buchanan, A. Chen, B.F. Du, E. Feric, M. Hierl, L.Y. Huang, D. Immke, B. Janosky, D. Johnson, X.W. Li, J. Ligutti, D. Liu, A. Malmberg, D. Matson, J. McDermott, P. Miu, H.N. Nguyen, V.F. Patel, D. Waldon, B. Wilenkin, X.M. Zheng, A.R. Zou, S.I. McDonough, E.F. DiMauro, Identification of a potent, state-dependent inhibitor of Nav1.7 with oral efficacy in the formalin model of persistent pain, *J. Med. Chem.* 54 (2011) 4427–4445.
- [26] H.L. Li, A. Galue, L. Meadows, D.S. Ragsdale, A molecular basis for the different local anesthetic affinities of resting versus open and inactivated states of the sodium channel, *Mol. Pharmacol.* 55 (1999) 134–141.
- [27] C.C. Kuo, L. Lu, Characterization of lamotrigine inhibition of Na⁺ channels in rat hippocampal neurons, *Br. J. Pharmacol.* 121 (1997) 1231–1238.
- [28] A. Al-Sabi, J. McArthur, V. Ostroumov, R.J. French, Marine toxins that target voltage-gated sodium channels, *Mar. Drugs* 4 (2006) 157–192.
- [29] T. Yasumoto, The chemistry and biological function of natural marine toxins, *Chem. Rev.* 1 (2001) 228–242.
- [30] A.L.R. Rentas, R. Rosa, A.D. Rodriguez, G.E. Demotta, Effect of alkaloid toxins from tropical marine sponges on membrane sodium currents, *Toxicol.* 33 (1995) 491–497.
- [31] A. Al-Mourabit, M.A. Zancanella, S. Tilvi, D. Romo, Biosynthesis, asymmetric synthesis, and pharmacology, including cellular targets, of the pyrrole-2-aminoimidazole marine alkaloids, *Nat. Prod. Rep.* 28 (2011) 1229–1260.
- [32] B. Forte, B. Malgesini, C. Piutti, F. Quartieri, A. Scolaro, G. Papeo, A submarine journey: the pyrrole-imidazole alkaloids, *Mar. Drugs* 7 (2009) 705–753.
- [33] T. Lindel, G. Breckle, M. Hochgurtel, C. Volk, A. Grube, M. Kock, Decomposition of oroidin in DMSO/TFA, *Tetrahedron Lett.* 45 (2004) 8149–8152.
- [34] C. Poverlein, G. Breckle, T. Lindel, Diels-Alder reactions of oroidin and model compounds, *Org. Lett.* 8 (2006) 819–821.
- [35] P.J. Dransfield, S.H. Wang, A. Dilley, D. Romo, Highly regioselective Diels-Alder reactions toward oroidin alkaloids: use of a tosylvinyl moiety as a nitrogen masking group with adjustable electronics, *Org. Lett.* 7 (2005), 4065–4065.
- [36] D.S. Ermolat'ev, E.V. Van der Eycken, A divergent synthesis of substituted 2-aminoimidazoles from 2-aminopyrimidines, *J. Org. Chem.* 73 (2008) 1679–1682.
- [37] A. Nudelman, Y. Bechor, E. Falb, B. Fischer, B.A. Wexler, A. Nudelman, Acetyl chloride–methanol as a convenient reagent for: a) quantitative formation of amine hydrochlorides b) carboxylate ester formation c) mild removal of *N*-t-Boc-protective group, *Synth. Commun.* 28 (1998) 471–474.